Two-Component Dendritic Gel: Effect of Spacer Chain Length on the Supramolecular Chiral Assembly

Andrew R. Hirst,[†] David K. Smith,*[,†] Martin C. Feiters,[‡] and Huub P. M. Geurts[§]

Department of Chemistry, University of York, Heslington, York, YO10 5DD, United Kingdom, Department of Organic Chemistry, University of Nijmegen, NSRIM, 1 Toernooiveld, NL-6525 ED Nijmegen, The Netherlands, and Department of General Instrumentation, University of Nijmegen, 1 Toernooiveld, NL-6525 ED Nijmegen, The Netherlands

Received May 19, 2004

The present study investigates in detail the physical gelation of toluene induced by the addition of simple aliphatic diamines to a dendritic L-lysine-based peptide. The gel-phase material obtained was characterized using differential scanning calorimetry, scanning electron microscopy, small-angle X-ray scattering, circular dichroism, ^{1}H NMR, and X-ray diffraction. When the length of the aliphatic diamine is incrementally increased (C6−C12), the thermally reversible gel−sol transition temperature is dramatically increased (4−105 °C). This paper shows that the molecular information preset in the diamine is transcribed into the supramolecular assembly on the microscale and that this, in turn, controls the highly tunable macroscopic materials properties. The results also demonstrate the importance of chirality in the assembly process and highlight the role played by the aliphatic diamine in modulating the transcription of chirality from the molecular to the microscopic level.

Introduction

The design of distinct molecular components that self-assemble into functional gel-phase materials has generated immense interest.[1] Self-assembly, underpinning nanoscale structure, reflects the individual components and the omnipresence of ordering as a result of multiple noncovalent interactions (i.e., hydrogen bonding, $\pi-\pi$ stacking, solvophobic effects, and van der Waals forces).[2] It has been recognized that nanoscale assemblies are analogous to macromolecules, with the repeat units linked to each other by noncovalent interactions (rather than covalent bonds) forming a network, which can be macroscopically expressed as gelation.[3] Increasingly, research efforts have focused on two-component gelators, which offer the potential of developing "soft" materials with highly tunable microscopic and macroscopic properties.[4−7] We previously communicated[8] the basic design principles of a two-component gelator based on the interaction of dendritic building blocks[9] with an aliphatic diamine (Figure 1). We reported the effects of molar concentration, molecular structure, and ratio of the two components on the gelation of an aprotic solvent (toluene). This full paper builds on our previous results, and by using new techniques such as small-angle X-ray scattering, circular dichroism, and variable temperature NMR, we can elucidate the precise mode of self-assembly (in terms of noncovalent interactions and packing arrangements) and relate the tunability of the aggregate morphology and mesoscale chirality directly to the spacer chain of the aliphatic diamine. It is hoped that the transfer of chirality from a single gelator unit into microscopic assemblies will provide an ideal platform for organic synthesis and chiral separations.[10]

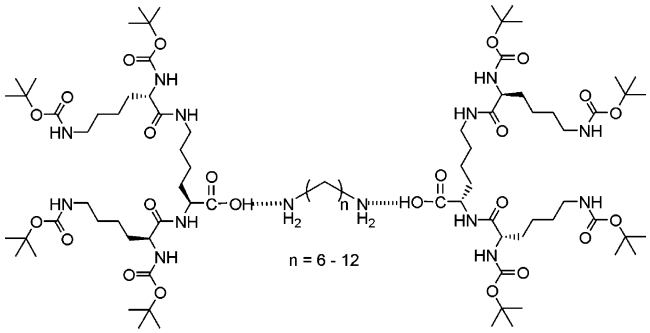

Figure 1. Structure of the dendritic two-component gelator unit.

* To whom correspondence should be addressed. E-mail: dks3@york.ac.uk.

† Department of Chemistry, University of York.

‡ Department of Organic Chemistry, University of Nijmegen.

§ Department of General Instrumentation, University of Nijmegen.

(1) (a) Terech, P.; Weiss, R. G. *Chem. Rev.* **1997**, *97*, 3133−3159. (b) Gronwald, O.; Snip, E.; Shinkai, S. *Curr. Opin. Colloid Interface Sci.* **2002**, *7*, 148−156. (c) van Esch, J. H.; Feringa, B. L. *Angew. Chem., Int. Ed.* **2000**, *39*, 2263−2266. (d) Oda, R.; Huc, I.; Candau, S. J. *Angew. Chem., Int. Ed.* **1998**, *37*, 2689−2691. (e) Abdallah, D. J.; Weiss, R. G. *Adv. Mater.* **2000**, *12*, 1237−1247. (f) Shimizu, T. *Polym. J.* **2003**, *35*, 1−22.

(2) (a) Whitesides, G. M.; Grzybowski, B. *Science* **2002**, *295*, 2418−2421. (b) Hamley, I. W. *Angew. Chem., Int. Ed.* **2003**, *42*, 1692−1712.

(3) Brunsveld, L.; Folmer, J. B.; Meijer, E. W.; Sijbesma, R. P. *Chem. Rev.* **2001**, *101*, 4071−4097.

(4) Two-component gels based on hydrogen bonding: (a) Hanabusa, K.; Miki, T.; Taguchi, Y.; Koyama, T.; Shirai, H. *J. Chem. Soc., Chem. Commun.* **1993**, 1382−1384. (b) Jeong, S. W.; Shinkai, S. *Nanotechnology* **1997**, *8*, 179−185. (c) Inoue, K.; Ono, Y.; Kanekiyo, Y.; Ishi-i, T.; Yoshihara, K.; Shinkai, S. *J. Org. Chem.* **1999**, *64*, 2933−2937. (d) Xu, X.; Ayyagari, M.; Tata, M.; John, V. T.; McPherson, G. L. *J. Phys. Chem.* **1993**, *97*, 11350−11353. (e) Tata, M.; John, V. T.; Waguespack, Y. Y.; McPherson, G. L. *J. Am. Chem. Soc.* **1994**, *116*, 9464−9470. (f) Waguespack, Y. Y.; Banerjee, S.; Ramannair, P.; Irvin, G. C.; John, V. T.; McPherson, G. L. *Langmuir* **2000**, *16*, 3036−3041. (g) Simmons, B. A.; Taylor, C. E.; Landis, F. A.; John, V. T.; McPherson, G. L.; Schwartz, D. K.; Moore, R. *J. Am. Chem. Soc.* **2001**, *123*, 2414−2421. (h) Willemen, H. M.; Vermonden, T.; Marcelis, A. T. M.; Sudhölter, E. J. R. *Langmuir* **2002**, *18*, 7102−7106. (i) de Loos, M.; van Esch, J.; Kellogg, R. M.; Feringa, B. L. *Angew. Chem., Int. Ed.* **2001**, *40*, 613−616. (j) Nakano, K.; Hishikawa, Y.; Sada, K.; Miyata, M.; Hanabusa, K. *Chem. Lett.* **2000**, 1170−1171.

(5) Two-component gels based on donor−acceptor interactions: (a) Maitra, U.; Kumar, P. V.; Chandra, N.; D'Sousa, L. J.; Prasanna, M. D.; Raju, A. R. *Chem. Commun.* **1999**, 595−596. (b) Friggeri, A.; Gronwald, O.; van Bommel, K. J. C.; Shinkai, S.; Reinhoudt, D. N. *J. Am. Chem. Soc.* **2002**, *124*, 10754−10758. (c) Babu, P.; Sangeetha, N. M.; Vijaykumar, P.; Maitra, U.; Rissanen, K.; Raju, A. R. *Chem.—Eur. J.* **2003**, *9*, 1922−1932.

10.1021/la048751s CCC: $27.50
Published on Web 07/21/2004

Results and Discussion

Synthesis. The L-lysine-based dendritic branches[11] (dendrons) were synthesized in optically pure form and in high yields, using a solution-phase approach previously reported by us,[12] with column chromatography being employed to isolate the purified material. The aliphatic diamines were purchased from Aldrich (C7, C8, C10, C12), Lancaster (C6, C9), and TCI-EP (C11).

Thermal Dependence of the Gel-Phase Materials: Tube Inversion and Differential Scanning Calorimetry. The building block or gelator unit that self-assembles, inducing macroscopic gelation of organic solvents, is shown in Figure 1. As previously reported, acid−base interactions between COOH and NH_2 play a crucial role in the assembly process.[8] To assess the structuring behavior of the different gelator units in toluene, the transition from an immobile to a mobile self-assembled state was determined by tube inversion experiments. This method served to define a mobile−gel transition temperature (i.e., a gel "boundary").[13] For the purpose of this discussion, the gel boundary is analogous to the thermally reversible gel−sol transition temperature (T_{gel}). All the gel-phase materials reported here were thermoreversible and optically clear, indicating good solubility of the two-component mixture under all conditions. Furthermore, all the gel-phase materials described here were formed using a 2:1 dendron/diamine ratio. Typically, as the molar concentration of the two-component gelator unit was increased, T_{gel} also increased until a "concentrated regime" was reached, denoted by a concentration-independent T_{gel}. Typically, this occurred at a dendron concentration of ~10 mM (see for example Figure 2). We define this concentration regime as the "plateau region".

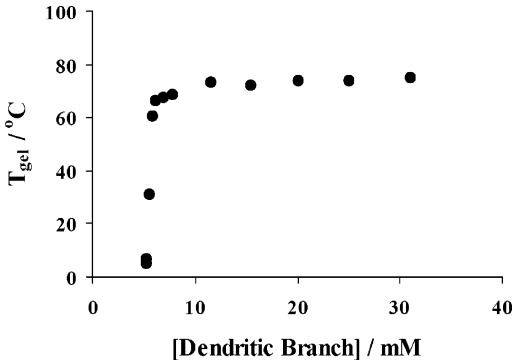

Figure 2. Effect of [dendritic branch] (diamine = C10) on the gel−sol transition temperature (T_{gel}).

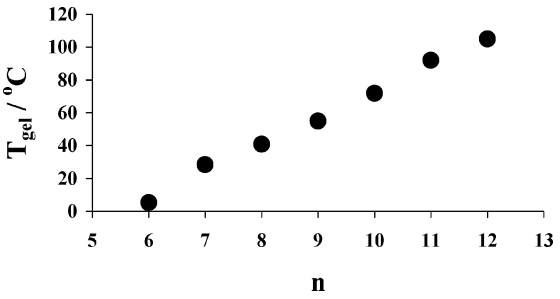

Figure 3. T_{gel} values (°C) versus n, the number of carbon atoms in the aliphatic diamine spacer chain. The solvent is toluene. [Dendritic branch] = 20 mM. [Aliphatic diamine] = 10 mM.

Increasing the length of the aliphatic spacer chain had a dramatic effect on the value of T_{gel} in the plateau region. As shown in Figure 3, the T_{gel} value increased linearly from 4 °C (C6) to 105 °C (C12). This means that by simple structural modification of the aliphatic spacer chain, self-complementary assembly of these gelator units (via van der Waals interactions and hydrogen bonding; see below) is meteorically enhanced.

In many cases, an odd−even effect of aliphatic chain length on gel properties is observed, an effect often related to packing effects of the aliphatic chains in the structured soft materials.[1f,14] In this case, however, the macroscopic gelation is not related to an odd−even effect conferred by the spacer unit. Decreasing the length of the aliphatic spacer chain renders these self-assemblies less susceptible to gelation, and below a critical spacer chain length (<C6) no macroscopic gelation was observed.

To obtain some information about the enthalpy change that accompanies the transition from an immobile self-assembled state to one that is mobile, differential scanning calorimetry (DSC) was employed. As shown in Figure 4, broad, prominent endothermic peaks were only observed in gel-phase materials possessing relatively long spacer chains (>C9). This reflects an increased level of order in the self-assembled state as the spacer unit was increased. The broadness of the peaks, however, typifies a less cooperative phase transition indicative of a system that is much less ordered than more crystalline structures.[15] The T_{gel} values obtained using the tube inversion method were compared to those collected using DSC. Generally, the tube inversion method provided T_{gel} values that are

(6) Two-component gels based on a reversible chemical reaction give rise to latent gels: (a) George, M.; Weiss, R. G. *Langmuir* **2003**, *19*, 1017−1025. (b) George, M.; Weiss, R. G. *Langmuir* **2002**, *18*, 7124−7135. Irreversible chemical reactions can also be used to generate gel-phase materials in situ: (c) Suzuki, M.; Nakajima, Y.; Yumoto, M.; Kimua, M.; Shirai, H.; Hanabusa, K. *Langmuir* **2003**, *19*, 8622−8624. (d) Suzuki, M.; Nakajima, Y.; Yumoto, M.; Kimura, M.; Shirai, H.; Hanabusa K. *Org. Biomol. Chem.* **2004**, *2*, 1155−1159.

(7) Two-component gels in which interaction of a ligand component with a metal ion modifies the properties of the gel-phase materials: (a) Ihara, H.; Sakurai, T.; Yamada, T.; Hashimoto, T.; Takafuji, M.; Sagaura, T.; Hachisako, H. *Langmuir* **2002**, *18*, 7120−7123. (b) Dukh, M.; Saman, D.; Kroulik, J.; Cerny, I.; Pouzar, V.; Kral, V.; Drasar, P. *Tetrahedron* **2003**, *59*, 4069−4076.

(8) (a) Partridge, K. S.; Smith, D. K.; Dykes, G. M.; McGrail, P. T. *Chem. Commun.* **2001**, 319−320. (b) Hirst, A. R.; Smith, D. K.; Feiters, M. C.; Geurts, H. P. M.; Wright, A. C. *J. Am. Chem. Soc.* **2003**, *125*, 9010−9011. We have also illustrated that this design principle can be applied to the formation of gels with the two components held together by interactions between a dendritic crown ether and a protonated aliphatic amine: (c) Dykes, G. M.; Smith, D. K. *Tetrahedron* **2003**, *59*, 3999−4009.

(9) For reports of one-component gels based on dendritic building blocks see: (a) Jang, W.-D.; Jiang, D.-L.; Aida, T. *J. Am. Chem. Soc.* **2000**, *122*, 3232−3233. (b) Jang, W.-D.; Aida, T. *Macromolecules* **2003**, *36*, 8461−8469. (c) Kim, C.; Kim, K. T.; Chang, Y.; Song, H. H.; Cho, T.-Y.; Jeon, H.-J. *J. Am. Chem. Soc.* **2001**, *123*, 5586−5587. (d) Marmillon, C.; Gauffre, F.; Gulik-Krzywicki, T.; Loup, C.; Caminade, A.-M.; Majoral, J.-P.; Vors, J.-P.; Rump, E. *Angew. Chem., Int. Ed.* **2001**, *40*, 2626−2629.

(10) Ihara, H.; Shudo, K.; Hirayama, C.; Hachisako, H.; Yamada, K. *Liq. Cryst.* **1996**, *20*, 807−809.

(11) For the original report of dendrimers based on L-lysine see: (a) Denkewalter, R. G.; Kolc, J.; Lukasavage, W. J. (Allied Corp.) U.S. Patent 4,289,872, 1981 [*Chem. Abstr.* **1985**, *102*, 79324q]. A number of other gel-phase materials based on L-lysine have been reported; see for example: (b) Hanabusa, K.; Nakayama, H.; Kimura, M.; Shirai, H. *Chem. Lett.* **2000**, 1070−1071. (c) Suzuki, M.; Yumoto, M.; Kimura, H.; Shirai, H.; Hanabusa, K. *Helv. Chim. Acta* **2004**, *87*, 1−10 and references therein.

(12) (a) Dykes, G. M.; Brierley, L. J.; Smith, D. K.; McGrail, P. T.; Seeley, G. J. *Chem.—Eur. J.* **2001**, *7*, 4730−4739. (b) Driffield, M.; Goodall, D. M.; Smith, D. K. *Org. Biomol. Chem.* **2003**, *1*, 2612−2620.

(13) (a) Chaibundit, C.; Shao-Min, M.; Heatley, F.; Booth, C. *Langmuir* **2000**, *16*, 9645−9652. (b) Kelarakis, A.; Yang, Z.; Pousia, E.; Nixon, S. K.; Price, C.; Booth, C.; Hamley, I. W.; Castelletto, V.; Fundin, J. *Langmuir* **2001**, *17*, 8085−8091.

(14) (a) Tomioka, K.; Sumiyoshi, T.; Narui, S.; Nagaoka, Y.; Iida, A.; Miwa, Y.; Taga, T.; Nakano, M.; Handa, T. *J. Am. Chem. Soc.* **2001**, *123*, 11817−11818. (b) Sumiyoshi, T.; Nishimura, K.; Nakano, M.; Handa, T.; Miwa, Y.; Tomioka, K. *J. Am. Chem. Soc.* **2003**, *125*, 12137−12142.

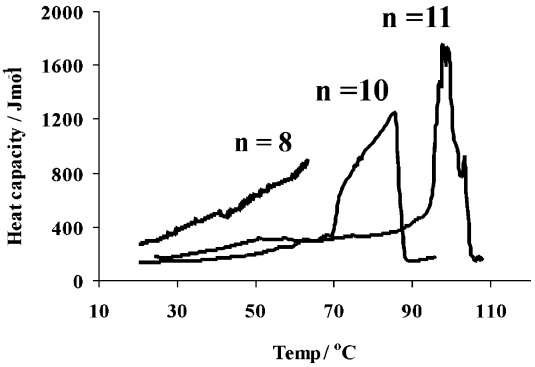

Figure 4. Differential scanning calorimetry data for two-component gels based on aliphatic diamines with different spacer lengths (*n*).

Table 1. Comparison of T_{gel} Values Obtained for Gels in Toluene Using Different Length Aliphatic Diamines $(NH_2(CH_2)_nNH_2)$[a]

n	T_{gel}/°C[b]	T_{onset}[c]	T_{max}[c]	T_{end}[c]	$\Delta H_{gel-sol}$/kJ mol^{-1}
9	55	60	73	82	13
10	72	70	85	88	16
11	92	95	99	107	20

[a] [Dendritic branch] = 20 mM, [aliphatic diamine] = 10 mM. $\Delta H_{gel-sol}$ values were estimated by integration of the area under the endothermic peak in the DSC trace. [b] Denotes values determined by the tube inversion method. [c] Denotes values determined using DSC.

in good agreement with the T_{onset} value determined by DSC (see Table 1). It has been shown previously that the gel to sol transition can be viewed in a manner similar to the dissolution of crystals allowing the relationship of T_{gel} with ΔH to be expressed in a Schrader relation.[16] However, the maximum in the DSC endothermic peak is ~15 °C higher than the transition point determined by the tube inversion method and therefore the evaluation of these data employing Schrader's equation is not valid in this case. It seems likely that the T_{gel} values determined by the tube inversion method relate to the temperature at which the number of "linkages" in the immobile gel drops below a critical network density.[17] In the case of the DSC measurement, a transition from a heterogeneous gel state to an isotropic self-assembled state is observed. We consider this transition to be related to the systematic breakdown of the sample-spanning network to smaller discrete aggregates.

The observed $\Delta H_{gel-sol}$ values were also estimated as a function of spacer chain length (Table 1) by simple integration of the endotherm. Interestingly, $\Delta H_{gel-sol}$ values were found to have some dependence on the spacer chain length. It is difficult to justify this large increase in enthalpy and T_{gel} values solely by considering individual van der Waals or solvophobic effects between the alkyl chains themselves, and this indicates that packing effects in the assembly may be a dominant feature.

Morphological Properties of the Gel Phase Materials: Scanning Electron Microscopy. Molecular self-assembly at the microlevel can be observed using scanning electron microscopy (SEM). This technique provides a comparative visual technique to assess the impact of the spacer unit on the mode of self-assembly. Figure 5A−D shows a series of SEM images of the organogels formed using various aliphatic diamines, solubilized by the same peptide-based dendritic peptide. The same concentration of gelator unit was employed in each case.

SEM revealed that the morphology of the self-assembled state is directly controlled by the length of the spacer unit. By incorporation of a relatively long spacer unit (i.e., C10, Figure 5A), thin fibers are observed, which self-assemble to form a bundle of fibers that together constitute an entangled network. The regular shape and high aspect ratio of the fibers are indicative of unidirectional stacking of gelator units, resulting in a one-dimensional mode of self-assembly.[1c] Therefore, we assume there is one-dimensional stacking of gelator units into fibers, which aggregate further into fiber bundles, and that this process immobilizes the isotropic aprotic solvent, hence inducing gelation. Analysis of the individual fibers shows that they are approximately 10 nm wide and several hundreds of nanometers long. This would indicate that the fiber is wider than the single two-component complex depicted in Figure 1.

Interestingly, decreasing the length of the spacer chain to C9 (Figure 5B) imparts a significant morphological change to the network structure even though the SEM is measured under the same conditions of gelator concentration. Although a highly directional self-assembled state is once again observed, the density of the network structure is considerably reduced from fiber bundles to a network that is composed of single fibers whose dimensions are approximately 30−40 nm wide with a polydispersity of lengths. It is easy to imagine from the SEM images that the loss of network density on the microscale will macroscopically manifest itself as a reduction in the degree of gelation. Further reduction of the length of the spacer chain to C8 (Figure 5C) results in the incremental loss of the fiberlike network. It is also apparent that the aspect ratio of the microstructure is considerably reduced and that the aggregates can be described as possessing a "fingerlike" morphology, rather than fibrous. For the organogel based on the C6 aliphatic spacer, a nonfibrous network is formed with no clear, well-defined microscale structure (Figure 5D). These findings imply that the molecular structure of the spacer unit directly controls the directionality of the aggregation process on the microscale and therefore the extent of fiber formation and the macroscopic properties of the gel.

We can, therefore, propose a mode of aggregation taking into account the various parameters: that is, the hydrogen bonded (acid−base) interaction, the spacer unit, and the dendritic peptide. The first step is the solubilization of the basic diamine spacer unit by the acidic dendritic peptide. It is important to note that this process has no directional organizational "power" in its own right. Solubilization (via acid−base interaction) is always achieved independent of the spacer chain length (remembering that in all cases the gel-phase materials under investigation are optically transparent). Second, under the nonpolar

(15) (a) Schoonbeek, F. S.; van Esch, J. H.; Hulst, R.; Kellogg, R. M.; Feringa, B. L. *Chem.—Eur. J.* **2000**, *6*, 2633−2643. (b) Hafkamp, R. J. H.; Feiters, M. C.; Nolte, J. M. *J. Org. Chem.* **1999**, *64*, 412−426. (c) van Esch, J. H.; de Feyter, S.; Kellogg, R. M.; de Schryver, F.; Feringa, B. L. *Chem.—Eur. J.* **1997**, *3*, 1238−1243.

(16) (a) Murata, K.; Aoki, M.; Suzuki, T.; Harada, T.; Kawabata, H.; Komori, T.; Ohseto, F.; Ueda, K.; Shinkai, S. *J. Am. Chem. Soc.* **1994**, *116*, 6664−6676. (b) Garner, C. M.; Terech, P.; Allegraud, J.; Mistrot, B.; Nguyen, P.; de Geyer, A.; Rivera, D. *J. Chem. Soc., Faraday Trans.* **1994**, *94*, 2173−2179. (c) Hanabusa, K.; Okui, K.; Karaki, K.; Koyama, T.; Shirai, H. *J. Chem. Soc., Chem. Commun.* **1992**, 1371−1373. (d) Terech, P.; Rossat, C.; Volino, F. *J. Colloid Interface Sci.* **2000**, *227*, 363−370. (e) Yoza, K.; Amanokura, N.; Ono, Y.; Akao, T.; Shinmori, H.; Takeuchi, M.; Shinkai, S.; Reinhoudt, D. N. *Chem.—Eur. J.* **1999**, *5*, 2722−2729. (f) Gronwald, O.; Sakurai, K.; Luboradzki, R.; Kimura, T.; Shinkai, S. *Carbohydr. Res.* **2001**, *331*, 307−318.

(17) This situation was first described by: (a) Eldridge, J. E.; Ferry, J. D. *J. Phys. Chem.* **1954**, *58*, 992−995. For a recent example see: (b) Brinksma, J.; Feringa, B. L.; Kellogg, R. M.; Vreeker, R.; van Esch, J. *Langmuir* **2000**, *16*, 9249−9255.

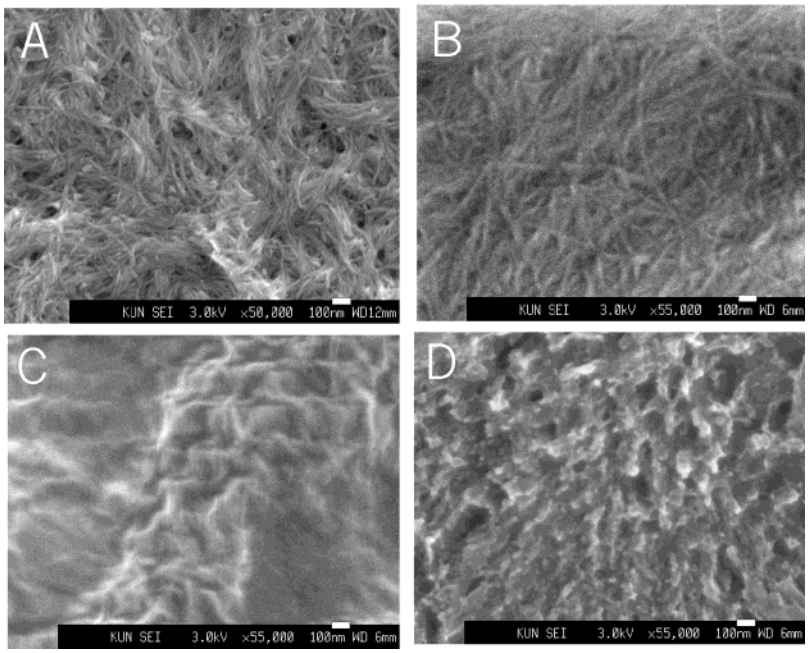

Figure 5. Effect of aliphatic chain length on aggregate morphology determined using SEM. [Dendritic branch = 10 mM]. (A) [C10] = 5 mM; (B) [C9] = 5 mM; (C) [C8] = 5 mM; (D) [C6] = 5 mM.

conditions as dictated by the choice of solvent (i.e., toluene) there is a strong driving force to orient the amide groups of the dendritic peptide in a mutually complementary array. This ordering process will maximize peptide−peptide self-assembly via intermolecular hydrogen bonding. However, the spacer unit appears to dictate the ability of the aggregated state to self-assemble in a unidirectional mode and therefore controls the ability of the peptides to form highly directional hydrogen bonding through their amide groups. Furthermore, increasing the aliphatic spacer chain allows the self-complementary arrangement of dendritic peptides to proceed in a more sterically favorable conformation. This maximizes the highly anisotropic nature of the amide hydrogen bond organization, giving rise to one-dimensional, hydrogen-bond-based fibers. This proposal is similar to previous models of the gelation properties of one-component systems (e.g., boronic acid appended bola amphiphiles with chiral diols[18] and bis-ureas[19]). This phenomenon is a rare example of controlling the morphology (i.e., the dimensionality) of the aggregated state by selecting simple building blocks with only slightly different structures.

Morphological Properties of the Gel-Phase Materials: Small-Angle X-ray Scattering. Small-angle X-ray scattering (SAXS) measurements of some selected materials in toluene showed reflections indicative of long-range order for all samples that were in the gel state. Interestingly, the study of the temperature dependence of the gel with 20 mM dendron and 10 mM C9 diamine revealed that the pattern broadens at the T_{gel} for this material (i.e., above 55 °C) and disappears altogether at higher temperatures (Figure 6, Table 2); this is strong evidence that the long-range order is indeed associated with gelation.

Variation of the spacer length resulted in varying patterns of X-ray reflections (Figure 7, Table 2), confirming

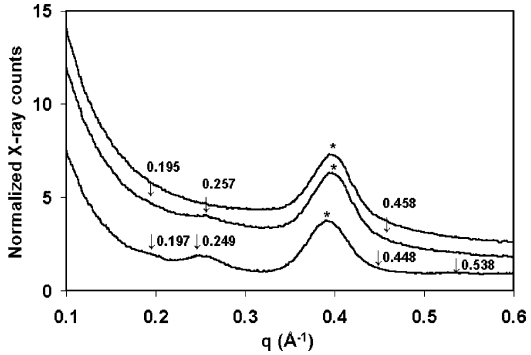

Figure 6. SAXS patterns of gels in toluene using a diaminononane spacer at different temperatures. Top, 70 °C; second from top, 55 °C; bottom, 25 °C. Arrows highlight peaks identified by peak fit (see also Table 2). An asterisk indicates an instrumental artifact.

Table 2. SAXS Peaks and Periodicities of Gels in Toluene of 20 mM Dendron with Various Aliphatic Diamine Spacers at Different Temperatures

spacer chain length, *n*	temperature/°C	peaks
12	25	0.199, 0.271, 0.475 Å^{-1} 31.6, 23.2, 13.2 Å
9	25	0.197, 0.249, 0.448, 0.538 Å^{-1} 31.9, 25.2, 14.0, 11.7 Å
8	25	0.156, 0.205, 0.249, 0.458 Å^{-1} 40.3, 30.6, 25.2, 13.7 Å
9	55	0.195, 0.257, 0.458 Å^{-1} 32.2, 24.4, 13.7 Å
9	70	no peaks

the importance of long-range order in all gels studied. However, although the periodicities might have been expected to increase with increasing chain length, no systematic variation of the positions of the reflections with spacer length was observed. Therefore, it was difficult to draw conclusions with regard to the packing of the molecules into fibers or the fibers into fiber bundles; the periodicities observed are of the order between that of packing of molecules into fibers and of fibers into fiber bundles. The wide-angle X-ray scattering (WAXS) region

(18) Koumoto, K.; Yamashita, T.; Kimura, T.; Luboradzki, R.; Shinkai, S. *Nanotechnology* **2001**, *12*, 25−31.

(19) van Esch, J.; Schoonbeek, F.; de Loos, M.; Veen, E. M.; Kellogg, R. M.; Feringa, B. L. *Supramolecular Science*: *Where It Is and Where It Is Going*; Ungaro, R., Dalcanale, E., Eds.; Kluwer: Dordrecht, 1999; pp 233−259.

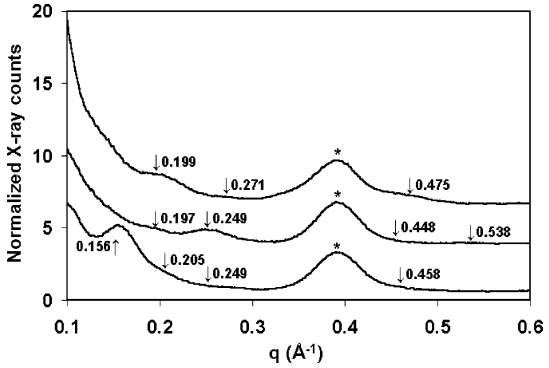

Figure 7. SAXS patterns of gels in toluene based on different diamine spacers. Top, $NH_2(CH_2)_{12}NH_2$; second from top, $NH_2(CH_2)_9NH_2$; bottom, $NH_2(CH_2)_8NH_2$. Arrows highlight peaks identified by peak fit (see also Table 2). An asterisk indicates an instrumental artifact.

(*d*: 5−1 Å, corresponding to the region of periodicities where reflections due to order in the molecular packing within the fibers might be expected) was also measured but no sharp reflections were observed. The patterns of reflections in the SAXS region could not be readily interpreted in terms of a common lamellar or hexagonal packing, such as observed in recent studies on 2,3-di-*n*-decyloxyanthracene in propylene carbonate[20] and methyl 4,6-*O*-benzylidene-α-D-mannopyranoside in *p*-xylene.[21] Analysis in terms of a packing of hollow cylinders such as performed for organogels of anthraquinone- and azobenzene-appended cholesterol derivatives[22] was not possible as our two-component gels do not have such contrasts in electron densities in their molecular structure. Although it proved impossible to interpret the diffraction patterns in terms of a molecular packing, the observation of such patterns is direct evidence for the order implied in our interpretation of our results of the thermal dependence and morphological studies.

Circular Dichroism Studies. Circular dichroism (CD) spectra[23] appear when the chromophoric moieties of chiral molecules are organized into an appropriate helical orientation.[24] It was possible that the inherent chirality present in the dendritic peptides and the specific orientation of the amide carbonyl groups in the fiber-forming process would allow the three-dimensional structure of the aggregated state to be studied.[7a,25] This indeed turned out to be the case. The investigation was performed in the dilute state (i.e., below the gelation threshold) in order to facilitate sample handling using cyclohexane as the aprotic solvent. Cyclohexane replaced toluene as the solvent of choice as it exhibits physical properties similar to those of toluene but importantly is UV "silent" across the wavelength region of interest (i.e., ∼220 nm). Cyclohexane was gelated by the two-component gelator at higher concentrations, and a paper providing a full description of all solvent effects on these gels is currently in preparation.

The effect of the aliphatic spacer chain on the helicity of the self-assembled state is shown in Figure 8A−D. The λ_{max} value of all CD peaks was observed at 222 nm, ascribable to the amide carbonyl group of the dendritic peptides. The CD peak for the self-assembled materials in cyclohexane can be assigned to the exciton coupling bands. This suggests that a "stacked" or helical arrangement is present in the self-assembled state, even below the gelation threshold. In each case, the CD band had the same negative sign, and this indicates that the bias in the supramolecular helix has the same directionality in each assembly.

Interestingly, however, the degree of helicity present in the self-assembled state was controlled by the length of the aliphatic spacer chain. All the CD spectra were measured at the same concentration of gelator complex ([dendritic branch] = 3 mM, [diamine] = 1.5 mM). Surprisingly, reducing the length of the spacer chain from C12 to C8 renders the aggregated state achiral even though the individual gelator units are composed of chiral centers. In addition, the CD results provide clear evidence that increasing the length of the spacer chain from C9 (Figure 8C) to C11 (Figure 8B) to C12 (Figure 8A) enhances chiral ordering (i.e., helicity) on the mesoscale. Tuning the aggregate helicity in this way is analogous to the "chiral bilayer effect" in which the stacking or aggregate "motif" is a result of a preferred packing of all the chiral centers.[26] However, in this case the dominant aggregate motif of the chiral peptides is controlled by the length of the aliphatic spacer chain rather than by a head-to-tail arrangement of chiral amphiphiles.

No CD signal was observed for the dendritic peptide alone in cyclohexane. This indicates that the negative CD signals are attributable to the increased helicity of the aggregated state, as dictated by the length of the aliphatic spacer chain, and not to the inherent chirality of the dendritic peptide. It was also confirmed that the contribution of linear dichroism (LD) to the true CD spectra is negligible.

^{1}H NMR Measurements. In general, NMR techniques can provide a large amount of information relating to the self-assembly of the gel state.[15a,16a,27] The ^{1}H NMR spectra of the d_8-toluene gels at room temperature were therefore recorded as a function of spacer unit. In each case, the ^{1}H NMR spectrum was measured in the plateau region with [dendritic branch] = 20 mM and [diamine] = 10 mM.

When the aliphatic spacer chain was increased in length, the resonance signals of the gelator unit, particularly the CH_3 of the *tert*-butyl groups, became markedly weaker. Thus, at room temperature, the self-assembled state becomes increasingly more rigid with increasing chain length. As a result, the signal intensities of the NH(1), NH(2), and NH(3) (carbamate) and the methylene protons

(20) Lescanne, M.; Colin, A.; Mondain-Monval, O.; Fages, F.; Pozzo, J.-L. *Langmuir* **2003**, *19*, 2013−2020.

(21) Sakurai, K.; Jeong, Y.; Koumoto, K.; Friggeri, A.; Gronwald, O.; Sakurai, S.; Okamoto, S.; Inoue, K.; Shinkai, S. *Langmuir* **2003**, *19*, 8211−8217.

(22) (a) Terech, P.; Ostuni, E.; Weiss, R. G. *J. Phys. Chem.* **1996**, *100*, 3759−3766. (b) Sakurai, K.; Ono, Y.; Jung, J. H.; Okamoto, S.; Sakurai, S.; Shinkai, S. *J. Chem. Soc., Perkin Trans. 2* **2001**, 108−112.

(23) For an overview of CD spectroscopy see: Berova, N.; Nakanishi, K.; Woody, R. W. *Circular Dichroism*: *Principles and Applications*, 2nd ed.; Wiley-VCH: Weinheim, 1994.

(24) For an example see: Hanabusa, K.; Okui, K.; Karaki, K.; Kimura, M.; Shirai, H. *J. Colloid Interface Sci.* **1997**, *195*, 86−93.

(25) For examples see: (a) Snip, E.; Shinkai, S.; Reinhoudt, D. N. *Tetrahedron Lett.* **2001**, *42*, 2153−2156. (b) Ihara, H.; Takafuji, M.; Sakurai, T.; Katsumoto, M.; Ushijima, N.; Shirosaki, T.; Hachisako, H. *Org. Biomol. Chem.* **2003**, *1*, 3004−3006. (c) Hanabusa, K.; Maesaka, Y.; Kimura, M.; Shirai, H. *Tetrahedron Lett.* **1999**, *40*, 2385−2388. (d) Goto, H.; Zhang, H. Q.; Yashima, E. *J. Am. Chem. Soc.* **2003**, *125*, 2516−2523. (e) van Gorp, J. J.; Vekemans, J. A. J. M.; Meijer, E. W. *J. Am. Chem. Soc.* **2002**, *124*, 14759−14769.

(26) (a) Fuhrhop, J. H.; Schnieder, P.; Rosenberg, J.; Boekema, E. *J. Am. Chem. Soc.* **1987**, *109*, 3387−3390. (b) Köning, J.; Böttcher, C.; Winkler, H.; Zeitler, Y.; Talmon, J. H.; Fuhrhop, J. H. *J. Am. Chem. Soc.* **1993**, *115*, 693−700.

(27) (a) Amanokura, N.; Yoza, K.; Shinmori, H,; Shinkai, S.; Reinhoudt, D. N. *J. Chem. Soc., Perkin Trans. 2* **1998**, 2585−2591. (b) Yoza, K.; Amanokura, N.; Ono, Y.; Akao, T.; Shinmori, H.; Takeuchi, M.; Shinkai, S.; Reinhoudt, D. N. *Chem.−Eur. J.* **1999**, *5*, 2722−2729. (c) Duncan, D. C.; Whitten, D. G. *Langmuir* **2000**, *16*, 6445−6452. (d) Tata, M.; John, V. T.; Waguespack, Y. Y.; McPherson, G. L. *J. Phys. Chem.* **1994**, *98*, 3809−3817. (e) Camerel, F.; Faul, C. F. J. *Chem. Commun.* **2003**, 1958−1959.

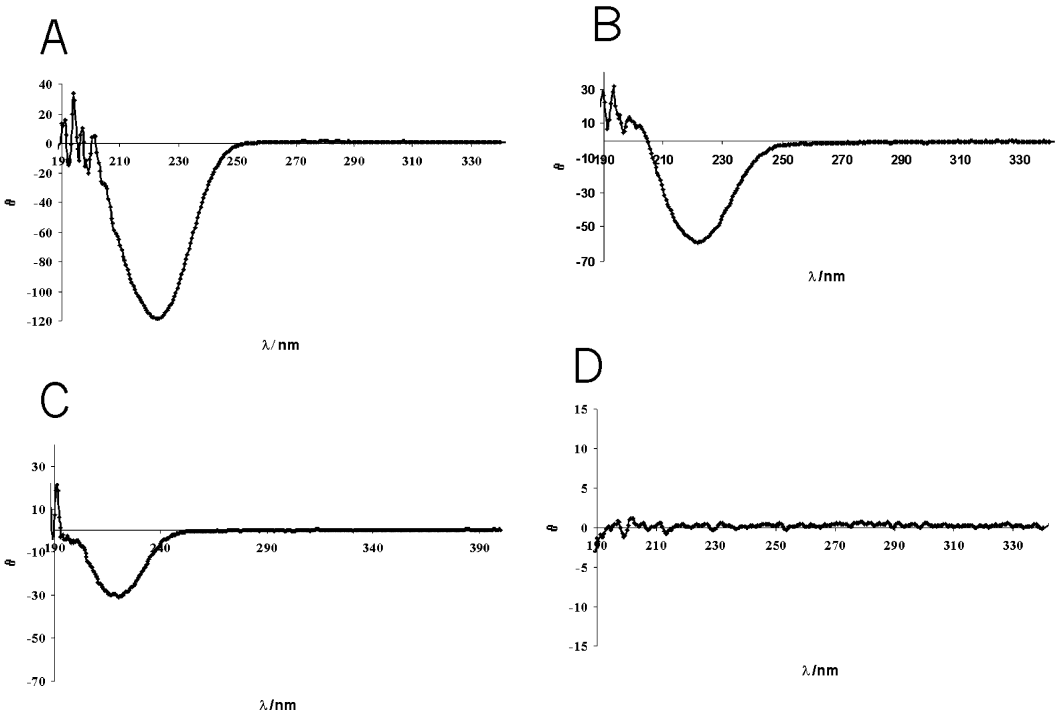

Figure 8. CD spectra of self-assembled materials (below the gelation threshold concentration) in cyclohexane at room temperature, [dendritic peptide] = 3 mM: (A) [C12] = 1.5 mM; (B) [C11] = 1.5 mM; (C) [C9] = 1.5 mM; (D) [C8] = 1.5 mM.

of the spacer unit ($\delta = 1.9$) all diminish to the point of nonobservability. We attribute this observation to the gelator units being held in an aggregated state so that their molecular motions are characterized by a time scale that is long compared to the NMR scale. Therefore, on the NMR time scale it became apparent that a self-assembly comprising a C6 spacer chain has more freedom of motion than other systems. This correlates with the macroscopic observations of the gel-forming abilities of the different spacer chains.

Interestingly, the resonances of the solvent (toluene) are present even in highly structured environments (i.e., C11- and C12-based gels) indicative of the solvent molecules retaining relatively unrestricted freedom of motion. This would be expected given that in the gel phase 98% of the material is "free" solvent, much of which will "sit" in open pockets within the mesoscale structure.

When the temperature was increased, the gelator signals became stronger, and upfield shifts were observed between 30 and 80 °C. A typical example is shown in Figure 9. The striking features of the resonances of NH(1) and NH(2) are the differences observed near the T_{gel} value. In this case, the T_{gel} was determined to be 55 °C ± 1. The resonances reached a maximum in intensity around this temperature. The temperature-dependent chemical shifts of easily identifiable protons were investigated, and in all cases, upfield shifts were observed. However, the NH protons showed a greater temperature dependency than the C*H, CH_2NH−, and CH_3 protons (see Supporting Information). This provides clear evidence that amide-based hydrogen bonding is the dominant feature required for gel formation. Presumably, the temperature-induced upfield shift of the NH protons is related to an increase in the electron density of the carbonyl oxygen atoms upon destruction of the hydrogen bonds. On increasing the temperature, the hydrogen bond interactions begin to break apart as entropy begins to dominate, hence resulting in the observed upfield shifts.

Increasing the molar concentration of the two-component gelator unit resulted in a concentration-induced

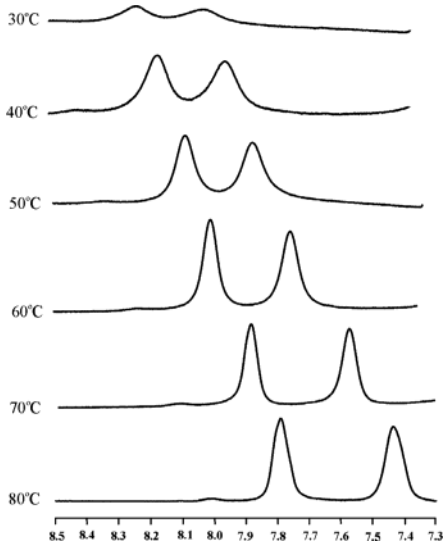

Figure 9. Effect of temperature on NH(1) and NH(2) resonances, [dendritic branch] = 20 mM, [C9] = 10 mM. NH(1) and NH(2) cannot be individually assigned, but they correspond to the two amide protons (not carbamates) within the second-generation L-lysine-based dendritic branch.

downfield shift of the NH protons (Figure 10). This trend is indicative of a self-assembly process driven by intermolecular hydrogen bonding. At a relatively high concentration (∼20 mM), a plateau region was reached, suggesting that an optimum number of intermolecular peptide−peptide hydrogen bonds were formed; this agrees directly with the measurement of macroscopic properties (i.e., T_{gel}) and unambiguously proves the crucial role of hydrogen bonding in mediating the assembly of the gel-phase materials.

The effect of spacer chain on the temperature-induced upfield shift of the NH protons was investigated. Interestingly, the effect of temperature was generally reduced (except for $n = 6$) as the length of the aliphatic spacer chain increased (Figure 11). In other words, increasing

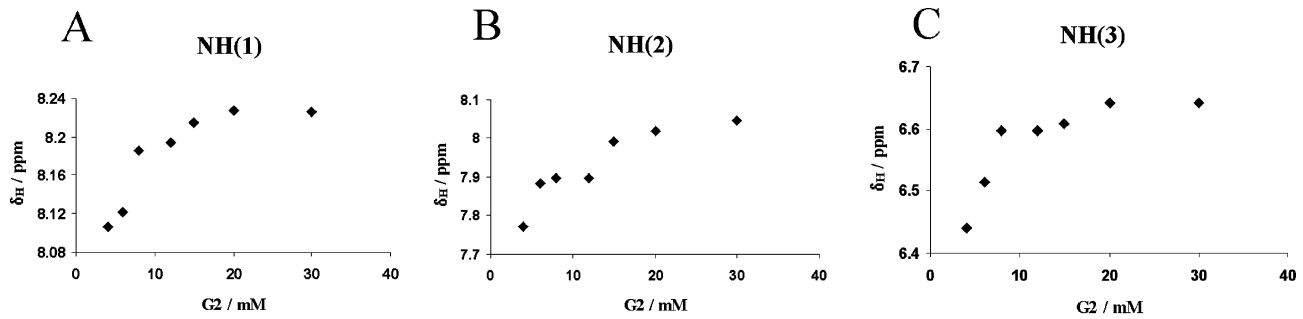

Figure 10. Effect of concentration on the resonances of different NH groups present in the dendritic branch, spacer chain length = C9, temperature = 30 °C. (A) NH(1) (amide); (B) NH(2) (amide); (C) NH(3) (carbamate).

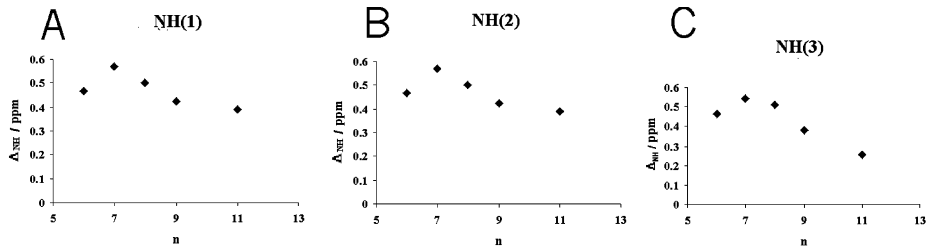

Figure 11. Effect of the spacer chain length (*n*) on the temperature-induced (30−80 °C) upfield shift of different NH protons: (A) NH(1) (amide); (B) NH(2) (amide); (C) NH(3) (carbamate). [Dendritic branch] = 20 mM, [C9] = 10 mM.

the temperature from 30 to 80 °C has a smaller effect with longer chain spacers. Therefore, we can infer that the binding strength within the aggregate (i.e., intermolecular amide hydrogen bonding) becomes increasingly stronger as the spacer length increases (i.e., temperature was less able to break down the mesoscale assemblies).

From CD and SEM studies, the most attractive packing arrangement for the gelator units appears to be a unidirectional stacked structure. Presumably, this leads to a more favorable alignment of hydrogen bonds. The strongest hydrogen bonds are those where the donor and acceptor are collinear.[28] Therefore, we propose that the aliphatic spacer chain modulates the degree of helicity present in the "stack" or self-assembled state and additionally controls the alignment and hence the binding strength of hydrogen bonding. The precondition for the formation of such molecular assemblies is intrinsically linked to the solubilization of the aliphatic diamine by the acidic dendritic peptide. Fundamentally, however, the length of the aliphatic chain governs the mesoscale self-assembly and ultimately the macroscopic gelation. One noticeable exception to this rule is the gelator unit comprising a C6 spacer. Surprisingly, the magnitude of temperature-induced upfield shift is smaller than for the C8 and C9 spacers even though macroscopic gelation is greater in the latter cases. This result suggests that in the case of the C6-based organogel, aggregates are formed that are stabilized via the misalignment of intermolecular amide hydrogen bonding. CD and SEM studies prove that the aggregates formed are not helical and that this system forms a nonfibrous network, indicative of a gel-phase material that has stable aggregates but forms a weak sample-spanning network. Hence, although the hydrogen bonding may be strong in this case, it does not give rise to the growth of unidirectional fibers required for effective gelation.

Experimental Section

Materials. The L-lysine-based dendritic branches[11] (dendrons) were synthesized in optically pure form and in high yields, using a solution-phase approach previously reported by us,[12] with column chromatography being employed to isolate the purified material. The aliphatic diamines were purchased from Aldrich (C7, C8, C10, C12), Lancaster (C6, C9), and TCI-EP (C11).

Gelation Experiments. The experiment was performed by solubilization of a weighted amount of dendritic gelator in a measured volume of selected pure solvent. The mixture was sonicated at ambient temperature for 30 min before heating and cooling produced a gel. The gel sample was left to stand overnight. Gelation was considered to have occurred when a homogeneous "solidlike" material was obtained that exhibited no gravitational flow. The thermally reversible gel−sol transition temperature (T_{gel}) was determined using a tube inversion methodology.

Differential Scanning Calorimetry. The thermograms were recorded on a SEIKO DSC 6200 instrument using closed stainless steel cups. The gelator was placed in the stainless steel cups, and the run was recorded (in triplicate). The scan speed for the heating cycle was 5 °C/min. Calibration was performed using a sapphire standard.

Scanning Electron Microscopy. Gel samples were applied to aluminum stubs and allowed to dry. Prior to examination, the gels were coated with a thin layer of gold/Pt (60:40). Scanning electron micrographs were recorded using a JEOL JSM-6330F instrument. Au/Pt deposition was performed using a Denton vacuum LLC.

Small-Angle X-ray Scattering. SAXS experiments were performed on the SAXS station at the Dutch−Belgian beamline (DUBBLE), BM 26, at the European Synchrotron Radiation Facility in Grenoble, France,[29] on organogels mounted in glueless sample cells developed for X-ray absorption spectroscopic studies in organic solvents.[30] SAXS data have been recorded with the gas multiwire two-dimensional detector at a sample-to-detector distance of 1.4 m, with an X-ray wavelength of 0.93 Å (13.27 eV). The SAXS data were successively normalized for absorption and detector uniformity and were radially averaged. Spatial calibration was reformed with silver behenate[31] with an estimated error margin of ±0.5% in the observed periodicities. The diffraction peaks as well as the background due to solvent scattering and an instrument artifact at $q = 0.4$ Å^{-1} were deconvoluted using Peakfit v4 (Jandel Scientific).

(28) Ludwig, R. *J. Mol. Liq.* **2000**, *84*, 65−75.

(29) Bras, W. *J. Macromol. Sci., Phys. B* **1998**, *37*, 557−565.

(30) Sprakel, V. S. I.; Feiters, M. C.; Nolte, R. J. M.; Hombergen, P. H. F. M.; Groenen, A.; de Haas, H. J. R. *Rev. Sci. Instrum.* **2002**, *73*, 2994−2998.

(31) Blanton, T. N.; Huang, T. C.; Toraya, H.; Hubbard, C. R.; Robie, S. B.; Louer, D.; Goebel, H. E.; Will, G.; Raftery, T. *Powder Diffr.* **1995**, *10*, 91−100.

Circular Dichroism Measurements. CD spectra were recorded in the far-ultraviolet region (200−350 nm) using a JASCO 810 spectrometer and a 1.0 mm quartz cuvette. A sample interval of 1 nm and an averaging time of 3 s were used in all experiments. [Dendritic branch] = 3 mM.

Variable Temperature ^{1}H NMR Measurements. ^{1}H NMR spectra were recorded on a JEOL 400 spectrometer. Chemical shifts are denoted in δ units (ppm) relative to toluene (^{1}H: δ = 7.16 ppm, δ = 2.1 ppm). All experiments were carried out with the following parameters: scan rate = 1000, relaxation time = 2 s.

Conclusions

Aliphatic diamines are solubilized by enantiomerically pure L-lysine-based dendritic peptides. These two-component systems exhibit gelling properties of aprotic organic solvents (e.g., toluene and cyclohexane) resulting in optically transparent and thermoreversible gels. The degree of structuring observed in these gel-phase materials is controlled by the length of the diamine spacer unit as illustrated by the thermally reversible gel−sol phase transition (T_{gel}). As the length of the spacer unit was increased incrementally from 6 to 12 carbon atoms, T_{gel} increased profoundly from 4 to 105 °C. To the best of our knowledge, there is no other gel-phase system that can rival this degree of materials tunability for such a simple structural change. Scanning electron microscopy showed that the length of the spacer unit dictated the aggregate morphology and that the formation of long, intertwined fibers with widths of 10−20 nm is a prerequisite for a high degree of structuring. This situation is only achieved with aliphatic diamines that possess longer spacer chains. Intriguingly, circular dichroism studies indicated that the spacer unit also controlled the level of helicity of the self-assembled state. Furthermore, ^{1}H NMR spectroscopy of the self-assembled state indicates that the spacer unit dictates the immobilization of the peptide units via intermolecular amide−amide hydrogen bonding, and it is proposed that in this way, the molecular structure of the spacer unit can directly control both the mesoscale morphology and the macroscopic properties of the gel. Further work investigating the effects of stereochemistry, solvent environment, and dendritic generation on the assembly process will be reported in due course, and in addition, work is in progress to develop applications for these highly tunable soft materials systems.

Acknowledgment. We thank the Leverhulme Trust for supporting this research through the provision of a postdoctoral fellowship (A.R.H.) and The Royal Society for funding a short-term visit travel grant (Ref 15939) to the University of Nijmegen, The Netherlands (A.R.H.). We also thank NWO (Dutch Research Council) for the provision of a travel grant and synchotron radiation facilities at DUBBLE as well as Dr. Igor P. Dolbnya for support.

Supporting Information Available: Effect of temperature on the resonances of different functional groups present in the dendritic branch. This material is available free of charge via the Internet at http://pubs.acs.org.

LA048751S